Complex *N*-Glycan and Metabolic Control in Tumor Cells

Richard Mendelsohn,[1] Pam Cheung,[1] Lloyd Berger,[1] Emily Partridge,[1,3] Ken Lau,[1] Alessandro Datti,[1] Judy Pawling,[1] and James W. Dennis[1,2,3]

[1]Samuel Lunenfeld Research Institute, Mount Sinai Hospital; Departments of [2]Medical Genetics and Microbiology and [3]Laboratory Medicine and Pathology, University of Toronto, Toronto, Ontario, Canada

Abstract

Golgi β1,6*N*-acetylglucosaminyltransferase V (Mgat5) produces β1,6GlcNAc-branched complex *N*-glycans on cell surface glycoproteins that bind to galectins and promote surface residency of glycoproteins, including cytokine receptors. Carcinoma cells from polyomavirus middle T (PyMT) transgenic mice on a Mgat5$^{-/-}$ background have reduced surface levels of epidermal growth factor (EGF) and transforming growth factor-β (TGF-β) receptors and are less sensitive to acute stimulation by cytokines *in vitro* compared with PyMT Mgat5$^{+/+}$ tumor cells but are nonetheless tumorigenic when injected into mice. Here, we report that PyMT Mgat5$^{-/-}$ cells are reduced in size, checkpoint impaired, and following serum withdrawal, fail to down-regulate glucose transport, protein synthesis, reactive oxygen species (ROS), and activation of Akt and extracellular signal-regulated kinase. To further characterize Mgat5$^{+/+}$ and Mgat5$^{-/-}$ tumor cells, a screen of pharmacologically active compounds was done. Mgat5$^{-/-}$ tumor cells were comparatively hypersensitive to the ROS inducer 2,3-dimethoxy-1,4-naphthoquinone, hyposensitive to tyrosine kinase inhibitors, to Golgi disruption by brefeldin A, and to mitotic arrest by colcemid, hydroxyurea, and camptothecin. Finally, regulation of ROS, glucose uptake, and sensitivities to EGF and TGF-β were rescued by Mgat5 expression or by hexosamine supplementation to complex *N*-glycan biosynthesis in Mgat5$^{-/-}$ cells. Our results suggest that complex *N*-glycans sensitize tumor cells to growth factors, and Mgat5 is required to balance responsiveness to growth and arrest cues downstream of metabolic flux. [Cancer Res 2007;67(20):9771–80]

Introduction

Oncogenic gain-of-function mutations in intracellular mediators of Ras/extracellular signal-regulated kinase (Erk) and phosphatidylinositol 3-kinase (PI3K)/Akt signaling stimulate cell proliferation and metabolism, thereby increasing growth autonomy by relaxing the requirements for extracellular growth factors. However, tumor cells remain dependent on extracellular cues, notably cytokines and substratum adhesion to polarize the cytoskeleton and promote epithelial-to-mesenchymal transition (EMT), a feature of invasive carcinomas (1). Epidermal growth factor (EGF) family of growth factors binds receptor tyrosine kinases (RTK) and activates PI3K/Erk signaling, glucose uptake, cell proliferation, and microfilament remodeling (2). TGF-β binding to TβRII promotes Par6-Smurf1–dependent degradation of RhoA in focal regions of polarized cells, which contributes to microfilament remodeling and the mesenchymal morphology (3). TGF-β activation of the canonical Smad2/Smad3 transcription factor pathway induces extracellular matrix production and, at high levels, inhibits cell cycle progression (4, 5). A balanced stimulation of RTK/Erk/PI3K and TβR/Smad2 pathways is required to sustain growth and avoid cell cycle arrest induced by the latter (6).

Galectin-3 binds to the *N*-glycans on cell surface receptors, which opposes their loss to endocytosis and enhances sensitivities to cognate ligands (7). The galectins are a family of β-galactoside–binding proteins that cross-link glycoproteins with avidities dependent on *N*-glycan structure and number (8). The number of *N*-glycans is a feature defined by the protein sequence of each glycoprotein, whereas *N*-glycan structures are determined by the Golgi *N*-glycan processing pathway and metabolite supply to sugar-nucleotide pools. Notably, fructose-6P, glutamine, and acetyl-CoA supply the hexosamine pathway for *de novo* UDP-*N*-acetylglucosamine (UDP-GlcNAc) biosynthesis, a rate-limiting substrate for *N*-acetylglucosaminyltransferases I, II, IV, and V [encoded by Mgat1, Mgat2, Mgat4a/b, and Golgi β1,6*N*-acetylglucosaminyltransferase V (Mgat5); refs. 9, 10]. These medial Golgi enzymes initiate antennae; their substitution by β1,4galactosyltransferase resulting in 0 to 4 (Galβ1,4GlcNAcβ1) antennae with proportionate increases in affinity for galectin-3. The physical and kinetic characteristics of the *N*-glycan branching pathway cooperate with the number of *N*-glycans to differentially regulate growth [e.g., EGFR receptor (EGFR)] and arrest (e.g., TGF-β) receptors at the cell surface downstream of metabolic flux to UDP-GlcNAc biosynthesis (8).

Mammary tumor cells derived from polyomavirus middle T (PyMT) transgenic mice on a Mgat5$^{-/-}$ background are less responsive to insulin-like growth factor (IGF), EGF, platelet-derived growth factor (PDGF), fibroblast growth factor (FGF), and TGF-β, with a reduced galectin-3 binding and shift receptors from the cell surface to the endosomes (7). The PyMT oncoprotein is a cytosolic adaptor protein that enhances PI3K/Akt–dependent membrane remodeling (11), which tends to reduce surface residency of glycoprotein receptors when the galectin lattice is weak. PyMT Mgat5$^{-/-}$ mice display reduced metastasis *in vivo* and tumor cells retain an epithelial morphology in culture, but expression of Mgat5 from a retroviral vector in PyMT Mgat5$^{-/-}$ tumor cells restores surface receptors, EMT, and the metastatic phenotype (7). Tumors arise in PyMT Mgat5$^{-/-}$ mice with a longer latency, but growth is observed in all mammary fat pads and often accelerated in the later stages, suggesting that there are genetic or epigenetic compensatory mechanisms (12).

Because RTKs are under tonic suppression by phosphatase in endosomes (13, 14), we examined the possibility that redox-dependent suppression of these phosphotyrosine phosphatases

Note: Supplementary data for this article are available at Cancer Research Online (http://cancerres.aacrjournals.org/).

R. Mendelsohn and P. Cheung are co-first authors.

Requests for reprints: James W. Dennis, Samuel Lunenfeld Research Institute, Mount Sinai Hospital, 600 University Avenue R988, Toronto, Ontario, Canada M5G 1X5. Phone: 416-586-4800, ext. 8233; Fax: 416-586-8588; E-mail: Dennis@mshri.on.ca.

doi:10.1158/0008-5472.CAN-06-4580

(PTP) might promote ligand-independent growth signaling in PyMT Mgat5$^{-/-}$ tumor cells. Leakage of electrons directly to O_2 from complexes I, III, and IV in the electron-transport chain generates superoxide ($O_2^{\cdot-}$), which is converted to H_2O_2 by superoxide dismutase. H_2O_2 titrates redox-sensitive proteins and, notably, oxidizes an essential thiol group found in the active site of PTPs (15). Examples include H_2O_2-mediated inhibition of PTEN, LAR, PTP1B, and LMW-PTP, which enhance positive downstream signaling (16–18). Oxidation of Cys^{124} in the active site of PTEN is reversible by thioredoxin/NADH (17). At focal sites of RTK activation, Rac1 is recruited to the NADPH-dependent oxidase (NOX) complex, which catalyzes H_2O_2 production (18). PDGF (19), EGF (20), and stromelysin (matrix metalloproteinase-3) stimulate Rac1/H_2O_2 and promote EMT in tumor cells (21). However, most of the reactive oxygen species (ROS) in mammalian cells are generated in the mitochondria (22). Elevated ROS in BCR-ABL–transformed cells are dependent on oncogenic activation of PI3K and mammalian target of rapamycin (mTOR), glucose uptake, and oxidative respiration (23). Overexpression of Mox1, a NADPH oxidase that catalyzes H_2O_2 production in a constitutive manner, is also transforming in NIH-3T3 cells (24). Herein, we show that glucose uptake and mitochondrial ROS production promotes growth signaling in PyMT Mgat5$^{-/-}$ tumor cells, compensating in part for cytokine insensitivity. Moreover, supplementation to complex *N*-glycan branching by Mgat5 expression or via the hexosamine pathway to UDP-GlcNAc promotes sensitivity to cytokines and control of glucose metabolism in tumor cells.

Materials and Methods

Cell lines. Tumor cell lines were established from spontaneous mammary carcinomas removed from PyMT transgenic mice on a 129sv × FVB background with either Mgat5$^{+/+}$ or Mgat5$^{-/-}$ genotypes (7, 12). Three independent PyMT Mgat5$^{-/-}$ cell lines and two PyMT Mgat5$^{+/+}$ were established and initial characterization revealed that the Mgat5$^{-/-}$ lines were less sensitive to cytokines and deficient in EMT. The cell lines Mgat5$^{+/+}$ (2.6), Mgat5$^{-/-}$ (22.9), and rescued Mgat5$^{-/-}$ (22.9) cells were characterized in more detail. For genetic rescue, Mgat5$^{-/-}$ (22.9) was infected with a pMX-PIE retroviral vector for expression of murine Mgat5 or Mgat5(L188R), a point mutation that blocks localization of the enzyme to the Golgi (25).

Western blots. Western blots were done on total cell lysates using antibodies to phospho-Erk (p-Erk) 1/2 kinase (Thr^{202}/Tyr^{204}; Sigma), phospho-Akt (p-Akt; Ser^{473}; Cell Signaling Technology), PTEN (Upstate Cell Signaling Solutions), Glut1 transporter (Chemicon), signal transducers and activators of transcription 1 (STAT1; Santa Cruz Biotechnology), phospho-STAT1 (Santa Cruz Biotechnology), elongation factor-2 (eEF2; Cell Signalling Technology), phospho-eEF2 (p-eEF2; Thr^{56}; Cell Signaling Technology), and γ-tubulin (Sigma).

Cell cycle fluorescence-activated cell sorting. For serum starvation experiments, 5 × 10^5 cells were plated per 10-cm tissue culture dish in fresh medium and cultured overnight, then washed with 1× PBS, and incubated for the indicated times with serum-free DMEM. For GlcNAc titration, subconfluent cells were conditioned for 48 h in DMEM, 10% fetal bovine serum (FBS), and GlcNAc at the indicated concentrations. At the indicated times, cells were trypsinized, washed in PBS before fixation with 80% ethanol, and held at 4°C until completion of experiment. Cells were washed in PBS and then in PBS, 12% Triton-X, and 0.12 mmol/L EDTA, followed by incubation with DNase-free RNase A (1 μg/mL) at 37°C for 30 min, and then stained with 50 μg/mL propidium iodide for 1 h in the dark. FACSCalibur and cell cycle profile analysis with ModFitLT version 3.0 software were used to analyze the cells. Tumor cell sizes were compared using forward scatter (FSC) measurements on the fluorescence-activated cell sorting (FACS) and with a Coulter counter.

Glucose transport and ATP. Cells were seeded in triplicate at 2.5 × 10^5 cells per well in six-well plates. Following incubation at 37°C, the cells were washed twice with assay buffer [Krebs-Ringer solution: 116 mmol/L NaCl, 5.4 mmol/L KCl, 0.8 mmol/L $MgSO_4$, 1.0 mmol/L $CaCl_2$, 25 mmol/L Tris-HCl, 0.2% bovine serum albumin, 1.0 mmol/L NaH_2PO_4, and 2.0 mmol/L Na_2PO_4 (pH 7.45)]. Then, assay buffer (1 mL/well) was added to each well and the cells were incubated at 37°C for 30 min, and then 1 mL of [^{3}H]2-deoxy-D-glucose (2 μCi/mL) in assay buffer was added to each well. The cells were incubated at 37°C for 20 min and washed four times with ice-cold assay buffer, and 0.5 mL of ice-cold 5% trichloroacetic acid (TCA) was added to each well. After 30 min on ice, 0.4 mL of TCA supernatant was removed and [^{3}H]2-deoxy-D-glucose was quantified by scintillation counting. ATP in cells at a density of 1,000 cells per well in 96-well plates (Corning 96 Flat White) was measured in triplicate, using the CellTiterGlo Luminescent Cell Viability Assay kit (Promega).

ROS measurements. Cells were seeded in triplicate at a density of 1,000 cells per well in 96-well plates (Corning 96 Flat Opaque). For drug incubations, cells were pretreated for 30 min with 10 μmol/L carbonyl cyanide *p*-(trifluoromethoxy) phenylhydrazone (FCCP; Sigma) or for 2 h with 5 mmol/L *N*-acetyl-cysteine (NAC; Sigma). The wells were washed with PBS, and 100 μL of a 1 μmol/L H_2DCFDA (Molecular Probes) in PBS were added. The probe diffuses into the cells and, on oxidation, becomes fluorescent and trapped in the cell. The plate was incubated at 37°C for 30 min and fluorescence intensity of the oxidized probe at the bottom of each well was measured with excitation at 485-20 nm and emission at 530-25 nm using the Analyst HT plate reader (Molecular Devices) and the Criterion Host software (LJL Biosystems). Background fluorescence in the absence of probe was subtracted, and a standard curve for oxidation was generated using hydrogen peroxide. Results are plotted as the mean ± SD of triplicate determination, and experiments were repeated thrice.

Translation rates. Cells were seeded in DMEM plus 10% FBS in triplicate at 2.5 × 10^5 cells per well in six-well plates. At the given time, the medium was discarded and the cells were washed twice with PBS. Each well was equilibrated with DMEM methionine-free medium for 30 min at 37°C, then medium was removed, and DMEM methionine-free medium with 20 μCi [^{35}S]methionine was added. The cells were treated for 30 min at 37°C. Following the incubation, the medium was removed and each well was washed twice with cold PBS, and then 200 μL of lysis buffer were added to each well. The cells were scraped from each well and then transferred to Eppendorfs. The samples were centrifuged at 14,000 × *g* for 10 min at 4°C. The supernatants were removed and 10% TCA was added on ice for 30 min, and then proteins were trapped on GF-C filters (Whatman). The filters were washed thrice with 10% TCA and then washed once with 96% ethanol. The filter papers were air dried and [^{35}S]methionine incorporation was quantified by scintillation counting.

Nuclear translocation of p-Erk and Smad2/3. Cells plated in 96-well plates at 1,000 cells per well for 24 h were serum starved for a further 24 h and then stimulated with TGF-β1, EGF, or FBS. Cells were fixed after 40 min of TGF-β stimulation to measure Smad2/3 nuclear translocation and cells were fixed after 5 min of EGF stimulation to measure p-Erk nuclear translocation. Cells were fixed for 10 min with 3.7% formaldehyde at 20°C, washed with PBS plus 1% FBS, and permeabilized using 100% methanol for 2 min. The cells were washed thrice and blocked in PBS plus 10% FBS overnight at 4°C. Mouse anti-Smad2/3 (Transduction Laboratories) or mouse p-Erk1/2 (Thr^{202}/Tyr^{204}; M-8159) was added at 1:1,000 in PBS plus 10% FBS for 2 h at 20°C. To measure nuclear phospho-p53 (Ser^{15}), cells were stained with antibodies (Cell Signaling Technology). The cells were washed thrice with PBS plus 1% FBS. Secondary antibody Alexa Fluor 488–labeled antimouse Ig (Molecular Probes) was added at 1:1,000 with Hoechst (1:2,000) for 1 h at 20°C. After washing thrice, the plates were scanned using the ArrayScan automated fluorescence microscope (Cellomics, Inc.). The nuclear staining intensity and cytoplasmic staining intensity were determined individually for 200 cells per well, and cytoplasmic staining intensity was subtracted from nuclear staining intensity for each cell. The mean ± SE (n = 200) was generally <4% at each assay point.

Differential sensitivities of Mgat5$^{+/+}$ and Mgat5$^{-/-}$ cells to chemicals. Mgat5$^{+/+}$ and Mgat5$^{-/-}$ tumor cells seeded at 750 per well in

96-well plates were cultured in DMEM and 1% FCS with each compound in the Sigma LOPAC(1280) library of pharmacologically active compounds at a final concentration of 5 μmol/L for 16 h. Drugs were added in duplicate wells using a BioMek-FX and incubated for 24 h, then 10 μL of AlamarBlue (Biosource) were added, and after a further 36 h at 37°C, plates were read using the Gemini XPS fluorometer (Molecular Devices) at 544 nm excitation/590 nm emission. The CellTiterGlo Luminescent Cell Viability Assay kit and the AlamarBlue assay produced similar results. Each plate contained eight positive (no cell treatment, PC) and eight negative (signal background, NC) controls. Data were normalized using the formula: $(FI_{sample} - \text{mean } FI_{NC}) / (\text{mean } FI_{PC} - \text{mean } FI_{NC}) \times 100$. "Hits" were defined as compounds associated with a signal that shifted by at least 3× SD from the mean of the entire sample population. The Z factors were 0.58 and 0.53 for the $Mgat^{+/+}$ and $Mgat^{-/-}$ screen, respectively, whereas the Z' factors were above 0.7 in both screen. Primary "hits" were subjected to confirmatory tests done in triplicate and by titration to compare IC_{50} values for $Mgat5^{+/+}$ and $Mgat5^{-/-}$ cells. The tyrosine kinase inhibitors AG835, PP2, and genistein were purchased from Calbiochem.

Results

Growth control in PyMT tumor cells is dependent on Mgat5. Serum-starved PyMT $Mgat5^{-/-}$ tumor cells show low levels of p-Erk nuclear translocation on addition of serum when compared with PyMT $Mgat5^{+/+}$ and Mgat5-rescued mutant cells (Fig. 1*A*). The $Mgat5^{-/-}$ tumor cells were smaller in size than $Mgat5^{+/+}$ tumor cells and rescued mutant cells, suggesting that Mgat5 and its *N*-glycan products may play a role in growth and cell cycle regulation (Fig. 1*B*). When injected s.c. into mice, $Mgat5^{+/+}$ and $Mgat5^{-/-}$ tumor cells grew at similar rates, indicating that reduced sensitivity to growth factors in $Mgat5^{-/-}$ cells does not restrict solid tumor cell growth (data not shown). Growth factor signal to PI3K/Akt/mTOR regulates protein synthesis and cell size, whereas growth factor signal to Erk and cyclin D/cyclin-dependent kinase 4/6 promotes G_1-S entry (26). $Mgat5^{-/-}$ cells in asynchronous cultures displayed an abnormal cell cycle profile with

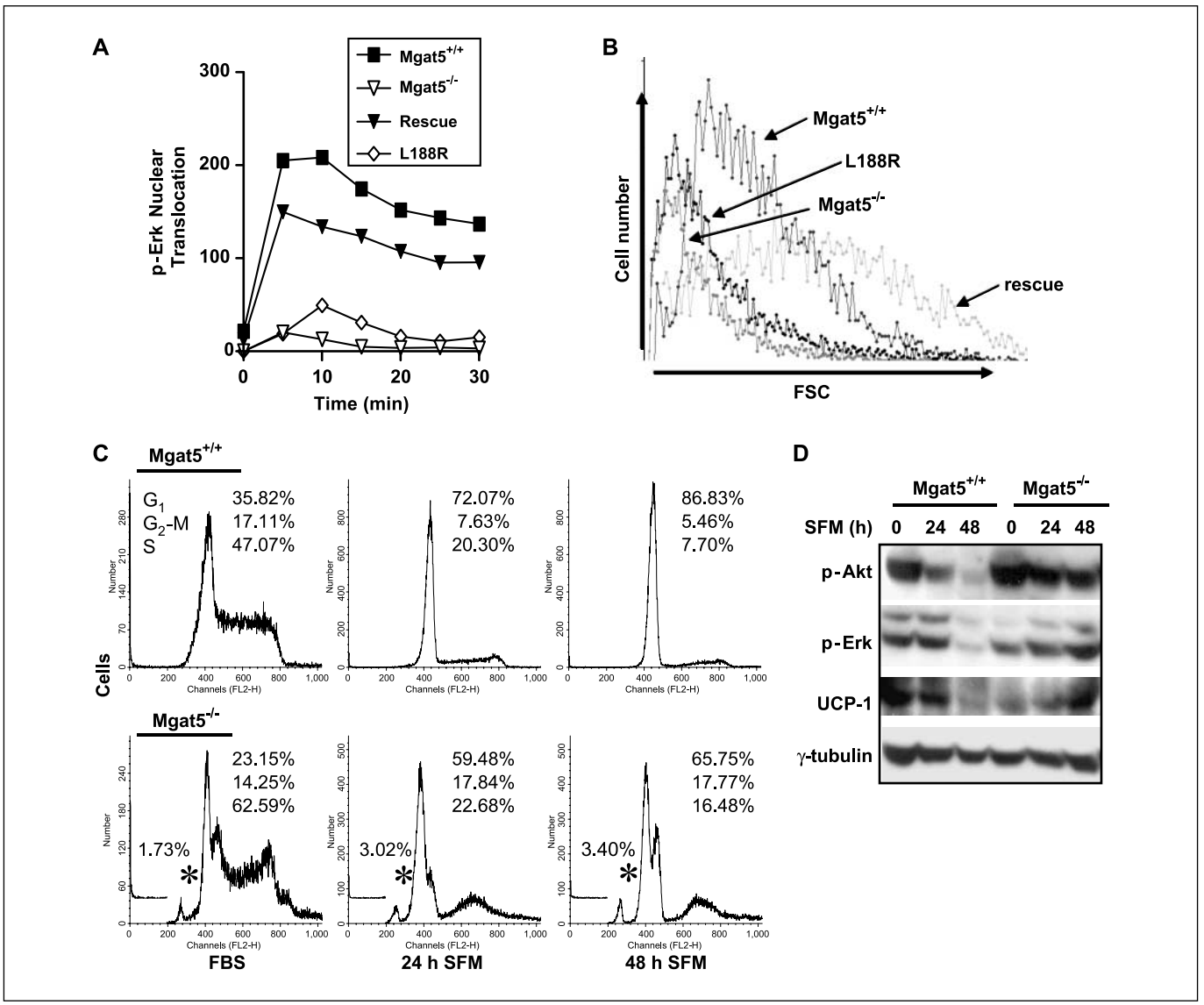

Figure 1. Altered growth signaling in Mgat5-deficient PyMT tumor cells. *A,* $Mgat5^{+/+}$ (2.6) and $Mgat5^{-/-}$ (22.9) tumor cells were serum starved for 24 h and stimulated with FBS, and p-Erk nuclear translocation was measured by ArrayScan. The "rescued" are $Mgat5^{-/-}$ (22.9) cells infected with a retrovial vector for expression of Mgat5 or the Mgat5 L188R mutant that does not localize to Golgi. *B,* tumor cells were grown in DMEM plus 10% FBS and cell size was measured by FSC. *C,* cell cycle distribution by FACS analyses following 0, 24, and 48 h of serum starvation. *D,* $Mgat5^{+/+}$ and $Mgat5^{-/-}$ tumor cells growing in DMEM plus 10% FBS were serum starved for the indicated times. Cell lysates were applied to SDS-PAGE and probed for p-Akt, p-Erk, UCP-1, and γ-tubulin.

increased apoptosis and a higher fraction of S and G_2-M phase cells compared with Mgat5$^{+/+}$ cells (Fig. 1*C*). More cells were observed in S-G_2-M after 48 h in serum-free medium (SFM) compared with Mgat5$^{+/+}$, reflecting a delay or failure of mutant cells to arrest in G_1 (Fig. 1*C*). p-Erk and p-Akt levels declined in Mgat5$^{+/+}$ cells 24 to 48 h after serum withdrawal but remained elevated in Mgat5$^{-/-}$ cells (Fig. 1*D*). Nuclear p53(Ser^{15}) levels were lower in Mgat5$^{-/-}$ tumor cells under normal growth conditions, consistent with a weakened checkpoint (Supplementary Fig. S1*A*). The M-phase blocker colcemid reduced growth of Mgat5-rescued mutant cells but not that of Mgat5$^{-/-}$ tumor cells (Supplementary Fig. S1*B*). Similarly, the S-phase blocker hydroxyurea slowed Mgat5-rescued cells but was less effective on Mgat5$^{-/-}$ tumor cells (Supplementary Fig. S1*C*). These experiments indicate that PyMT Mgat5$^{-/-}$ cells are functionally deficient in G_1-S and G_2-M checkpoints and suggest that shorter pauses in interphase result in reduced cell size.

Mgat5- and PyMT-dependent control of metabolism. Although PI3K/Akt activation is known to stimulate glucose uptake (27), we explored the converse relationship: whether hyperglucose metabolism in Mgat5$^{-/-}$ cells contributes to PI3K/Akt signaling. Glucose uptake rates were similar in Mgat5$^{+/+}$, Mgat5$^{-/-}$, and Mgat5-rescued cell lines cultured in serum-containing medium, but after 24 h in SFM, Mgat5$^{+/+}$ and Mgat5-rescued cells showed strong down-regulation, whereas glucose uptake remained unchanged in Mgat5$^{-/-}$ cells at 24 h and showed an increase by 72 h (Fig. 2*A*). *GLUT1* gene expression is increased by oncogenic transformation of cultured cells and correlates with poor survival of cancer patients (28). Glut1 protein levels were 2- to 3-fold higher in Mgat5$^{-/-}$ cells compared with Mgat5$^{+/+}$ cells (Fig. 2*B*). Glucose transport V_{max} was 6-fold higher in Mgat5$^{-/-}$ compared with Mgat5$^{+/+}$ cells, whereas K_D values were similar indicating that Mgat5-dependent *N*-glycosylation did not alter the kinetics of transport (Fig. 2*C*). After 24 h in SFM, ROS levels decreased in Mgat5$^{+/+}$ tumor cells but increased 2-fold in Mgat5$^{-/-}$ tumor cells (Fig. 2*D*). We might expect the Mgat5 deficiency in surface RTKs to reduce basal growth signaling and suppress glucose uptake in the absence of PyMT oncoprotein. Indeed, Mgat5$^{-/-}$ mouse embryonic fibroblasts (MEF) proliferate more slowly and display reduced sensitivity to EGF, PDGF, FGF, and IGF (29). Glucose uptake and ROS levels were reduced in Mgat5$^{-/-}$ MEFs compared with Mgat5$^{+/+}$ MEFs (Supplementary Fig. S2*A* and *B*; ref. 29). Serum withdrawal further reduced glucose uptake and ROS in both mutant and wild-type (WT) MEFs. Taken together, this suggests that Mgat5 promotes growth signaling and glucose

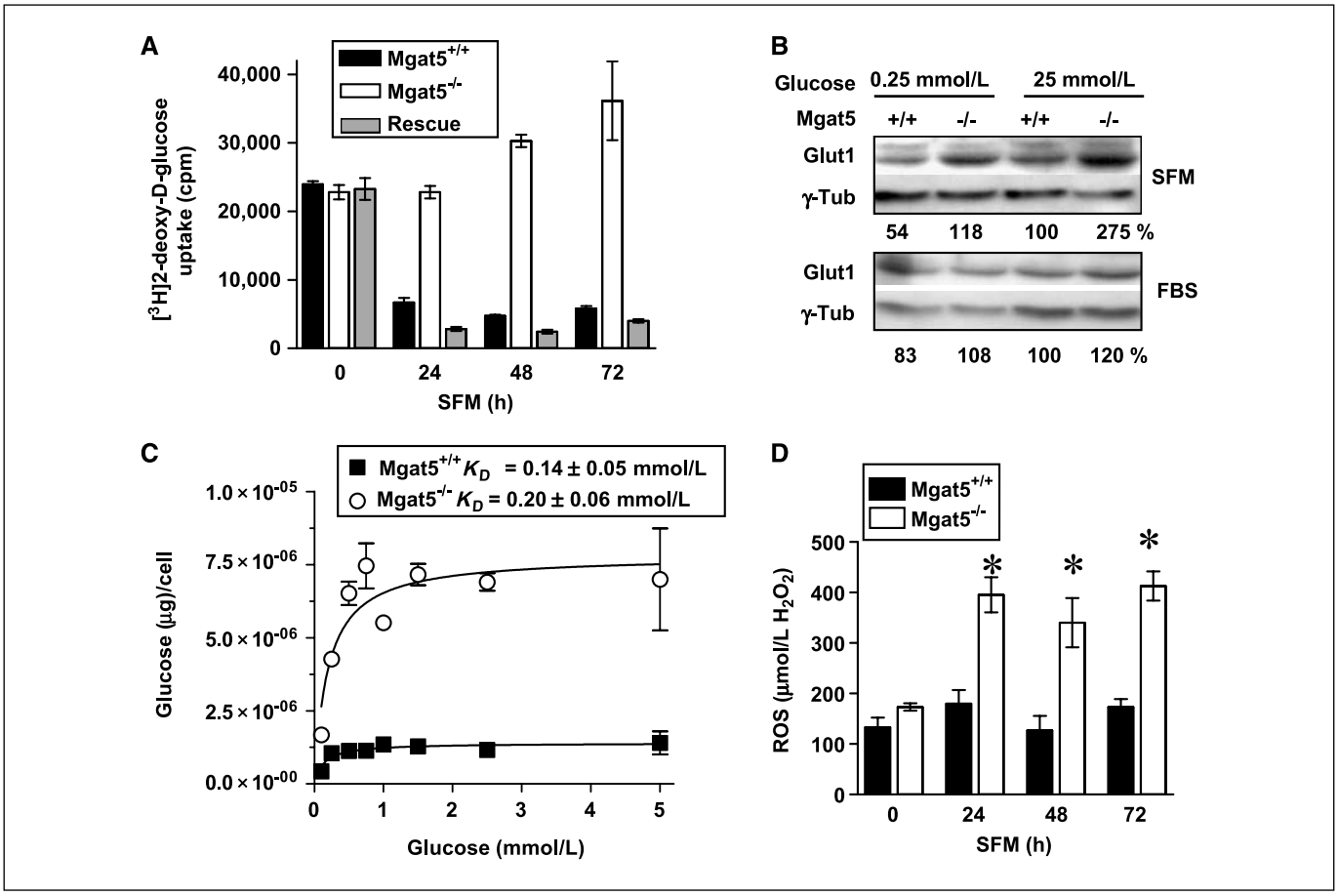

Figure 2. Mgat5-dependent regulation of glucose uptake in tumor cells and MEFs. Experiments were done with cells grown in DMEM containing 25 mmol/L glucose unless otherwise noted. *A,* Mgat5$^{+/+}$, Mgat5$^{-/-}$, and Mgat5-rescued tumor cells cultured in DMEM plus 10% FBS were serum starved for 0, 24, or 48 h, and [^{3}H]2-deoxy-D-glucose uptake was measured 20 min after addition. Representative of three experiments. *Columns,* mean of triplicates; *bars,* SE. $P < 0.05$ by ANOVA. *B,* Western blot of cell lysates for Glut1 glucose transporter and γ-tubulin (*γ-Tub*). Cells grown in DMEM ± FBS and with either 25 or 0.25 mmol/L glucose for 24 h. *C,* [^{3}H]2-deoxy-D-glucose tracer measuring glucose transport in Mgat5$^{+/+}$ and Mgat5$^{-/-}$ tumor cells following 24 h in SFM. *D,* ROS levels at 0, 24, 48, or 72 h after serum withdrawal. Mean of triplicate measurements. *, $P < 0.05$ by paired *t* test.

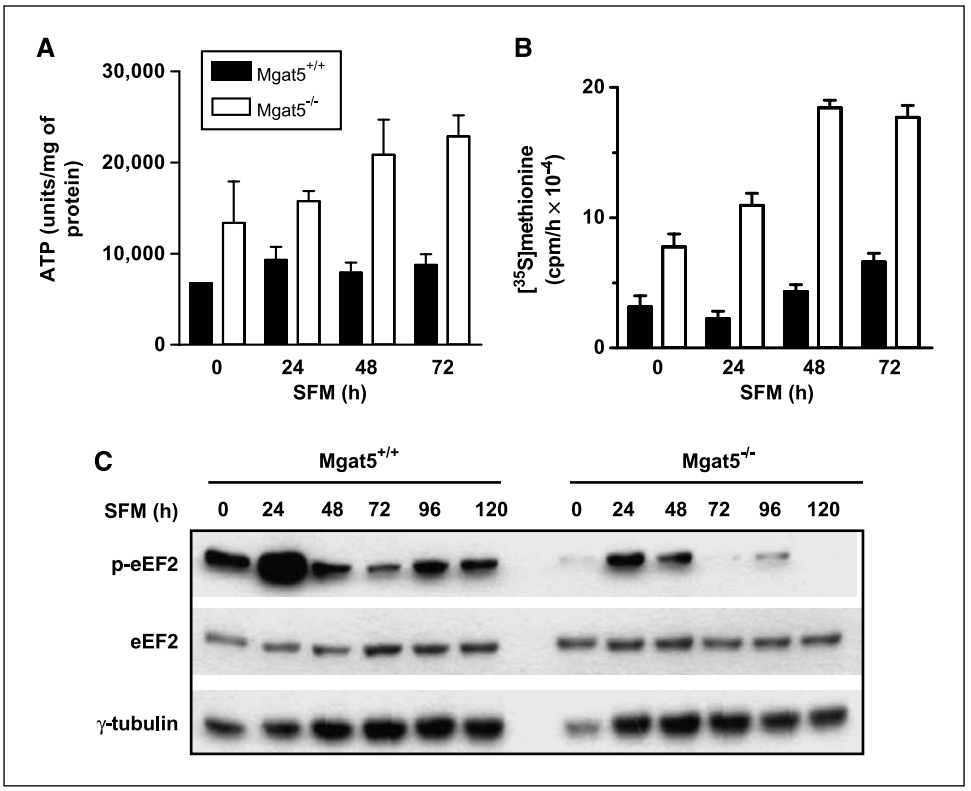

Figure 3. Mgat5-dependent regulation of growth signaling, oxidative phosphorylation, and protein synthesis. *A,* ATP levels in cell lysates. Representative of three experiments. *Columns,* mean; *bars,* SE. $P < 0.05$ by paired *t* test. *B,* [^{35}S]methionine incorporation into protein following a 30-min pulse labeling. Representative of three experiments. *Columns,* mean; *bars,* SD. $P < 0.05$ by paired *t* test. *C,* Western blot of cell lysates probed for Thr^{56} p-eEF2 and γ-tubulin.

uptake in nontransformed cells, but this requirement is removed by the PyMT oncoprotein, which drives a glucose-dependent positive feedback loop. However, Mgat5 expression seems to be required in PyMT-transformed cells to sense serum withdrawal and suppress growth.

Translational initiation and elongation are positively regulated by Akt/mTOR and inhibited by AMP-activated protein kinase (AMPK; refs. 30, 31). ATP levels were 2-fold higher in Mgat5$^{-/-}$ cells and increased further upon transfer to SFM, whereas ATP was unchanged in Mgat5$^{+/+}$ cells (Fig. 3*A*). Mgat5$^{-/-}$ cells displayed a higher rate of [^{35}S]methionine incorporation into proteins, which increased after serum withdrawal at a faster rate than that observed in Mgat5$^{+/+}$ cells (Fig. 3*B*). Pdk1 activates mTOR, and in turn S6 kinase, which phosphorylates eEF2 at Ser^{366}, thus activating protein translation. Serum withdrawal leads to inactivation of eEF2 by dephosphorylation at Ser^{366} and phosphorylation at Thr^{56} (32, 33). A comparison of Mgat5$^{-/-}$ and Mgat5$^{+/+}$ cells growing in serum-containing medium revealed that the basal rate of protein synthesis was higher and Thr^{56} p-eEF2 levels lower in mutant cells (Fig. 3*B* and *C*). After 24 h of SFM, Mgat5$^{+/+}$ cells showed a marked increase in Thr^{56} p-eEF2, accompanied by a small decline in protein synthesis. Although Thr^{56} p-eEF2 also increased in Mgat5$^{-/-}$ cells at 24 h of SFM, it did not reach levels observed in Mgat5$^{+/+}$cells, presumably remaining below a threshold for protein synthesis inhibition. Thr^{56} p-eEF2 decreased between 24 and 72 h in SFM for both Mgat5$^{-/-}$ and Mgat5$^{+/+}$ cells, accompanied by increased rates of protein synthesis. Thus, PyMT Mgat5$^{-/-}$ tumor cells in normal and SFM growth conditions maintain a higher energy charge and protein synthesis rate.

ROS-dependent Erk/Akt signaling in Mgat5$^{-/-}$ cells. Next, we examined the relationship between elevated metabolism in Mgat5$^{-/-}$ cells and growth signaling. The excess ROS in Mgat5$^{-/-}$ tumor cells growing in SFM was suppressed by treating cells for 30 min with carbonyl cyanide FCCP, an uncoupler of oxidative phosphorylation (Fig. 4*A*). NAC, a thiol reductant, also suppressed ROS in Mgat5$^{-/-}$ cells. FCCP treatment reduced tonic p-Akt and p-Erk in Mgat5$^{-/-}$ cells to levels comparable with that of untreated Mgat5$^{+/+}$ cells in SFM conditions (Fig. 4*B*). Mgat5$^{-/-}$ cells treated with rapamycin, an mTOR inhibitor, displayed a decrease in ROS production, whereas glucose uptake was reduced by treatment with rapamycin or the PI3K inhibitor LY294002 (Fig. 4*C* and *D*). ROS levels were unaffected in Mgat5$^{+/+}$ cells, whereas glucose uptake was reduced by LY294002. This indicates that high ROS production in Mgat5$^{-/-}$ cells is dependent in part on PI3K/mTOR activation of metabolism. Mitochondrial ROS is suppressed by the uncoupling proteins (UCP), which catalyze a controlled leakage of protons across the inner membrane. UCP-1 levels were lower in Mgat5$^{-/-}$ tumor cells than Mgat5$^{+/+}$ cells, and following serum withdrawal, UCP-1 increased in Mgat5$^{-/-}$ tumor cells and decreased in Mgat5$^{+/+}$ cells (Fig. 1*C*). UCP-1 expression is stimulated by superoxides (22), which may provide negative feedback to suppress mitochondrial ROS production.

ROS stimulates antioxidant pathways that limit damage (34), suggesting the possibility that high ROS levels in Mgat5$^{-/-}$ cells may be coupled with higher turnover rates for signaling intermediates. To examine this possibility, we compared the recovery rates of p-Erk, p-Akt, and oxidized PTEN following a pulse of exogenous H_2O_2. Akt became highly phosphorylated in both Mgat5$^{+/+}$ and Mgat5$^{-/-}$ within 20 min of H_2O_2 addition, and the return to baseline was marginally more rapid in Mgat5$^{-/-}$cells, as was the recovery of reduced PTEN in Mgat5$^{+/+}$ and Mgat5$^{-/-}$ (Fig. 5*A*). However, Erk phosphorylation recovered more rapidly in Mgat5$^{-/-}$ compared with Mgat5$^{+/+}$ tumor cells in SFM conditions (Fig. 5*B*). This suggests that anti-oxidant pathways

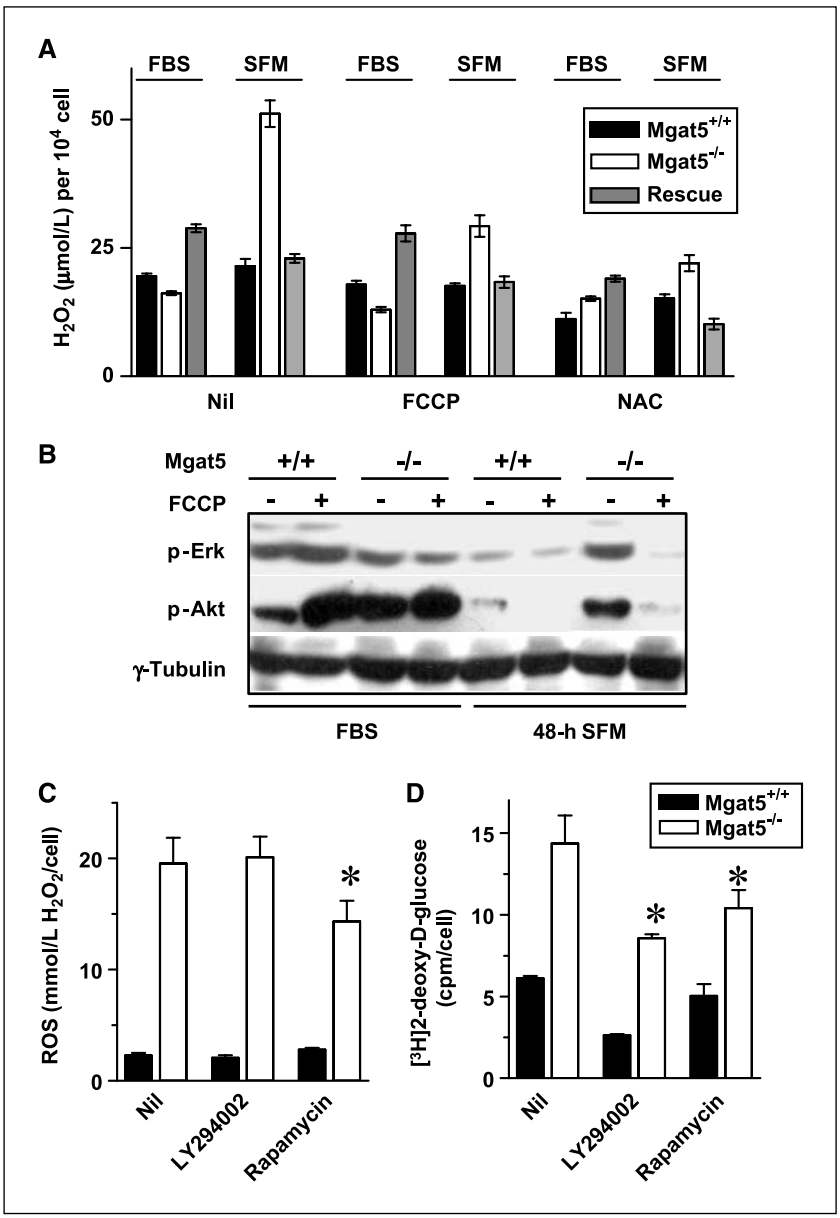

Figure 4. Mitochondrial ROS production and growth signaling in Mgat5$^{-/-}$ tumor cells. *A,* ROS levels in Mgat5$^{+/+}$, Mgat5$^{-/-}$, and Mgat5-rescued cells. Cells were either untreated or pretreated with 10 μmol/L FCCP for 30 min or with 5 mmol/L NAC for 2 h. $P < 0.05$ by ANOVA. *B,* Mgat5$^{+/+}$ and Mgat5$^{-/-}$ cells growing in DMEM with and without FBS for 48 h were either untreated or treated with 10 μmol/L FCCP for 30 min. Western blot probed for p-Akt, p-Erk, and γ-tubulin. *C* and *D,* Mgat5$^{+/+}$ and Mgat5$^{-/-}$ cells growing in DMEM without FBS for 48 h and treated with the LY294002 or rapamycin for 3 h before measuring ROS and glucose uptake.

are also increased in Mgat5$^{-/-}$ cells and contribute to increased steady-state and turnover rates of p-Akt and p-Erk. The activity of ROS as a PTP inhibitor may render Mgat5$^{-/-}$ cells less dependent on specific membrane RTKs. Indeed, Mgat5$^{-/-}$ cells were 5 times more resistant to PP2, an inhibitor of Src family kinases, 10 times more resistant to genistein, a broad range tyrosine kinase inhibitor, and 3-fold more resistant to AG835, an inhibitor of EGFR (Fig. 5*C*).

To further explore the critical determinant of growth in an unbiased manner, we screened the LOPAC chemical library for compounds with differential effects on growth of Mgat5$^{-/-}$ and Mgat5$^{+/+}$ tumor cells. Only 3 of 1,200 compounds met this criterion. Mgat5$^{-/-}$ cells were more sensitive to 2,3-dimethoxy-1,4-naphthoquinone (DMNQ), a ROS inducer (Fig. 5*D*). DMNQ induced ~2-fold higher levels of H_2O_2 in Mgat5$^{-/-}$ cells than in Mgat5$^{+/+}$ cells consistent with differential toxicity (data not shown). Mgat5$^{+/+}$ cells were also more sensitive to brefeldin A, which disrupts Golgi, and to camptothecin, a topoisomerase inhibitor. These results are consistent with the defect observed in Mgat5$^{-/-}$ cells, notably increased oxidative stress, reduced dependency on complex *N*-glycan, and reduced checkpoint enforcement. Greater resistance to kinase inhibitors suggests that growth and survival in Mgat5$^{-/-}$ cells are more dependent on redox turnover than extracellular cytokines.

Rescue of metabolic control in Mgat5$^{-/-}$ cells by hexosamine supplementation. Our results suggest that growth signaling in PyMT Mgat5$^{-/-}$ tumor cells is less dependent on cytokines and more dependent on positive feedback from glucose metabolism. Mgat5$^{-/-}$ tumor cells fail to down-regulate growth in SFM, suggesting that β1,6GlcNAc-branched *N*-glycans may also be required to suppress growth signaling. *N*-glycan branching is increased with GlcNAc supplementation to the culture medium, and this enhances galectin-dependent binding and retention of receptor at the cell surface (8). GlcNAc is salvaged by the

hexosamine pathway and increases UDP-GlcNAc supply to Golgi *N*-acetylglucosaminyltransferases (Mgat1, Mgat2, Mgat4a/b, and Mgat5; Supplementary Fig. S3*A*). GlcNAc supplementation does not restore β1,6GlcNAc-branched *N*-glycans in Mgat5$^{-/-}$ cells but rather increases the fraction of the next most branched *N*-glycan (tri-antennary) from 15% to 30% of the total *N*-glycan pool (8). The tri-antennary and tetra-antennary *N*-glycans in Mgat5$^{+/+}$ cells increase only marginally with GlcNAc supplementation, suggesting that the medial Golgi pathway in Mgat5$^{+/+}$ tumor cells is operating closer to saturation for UDP-GlcNAc (8). Activation of PI3K and Erk

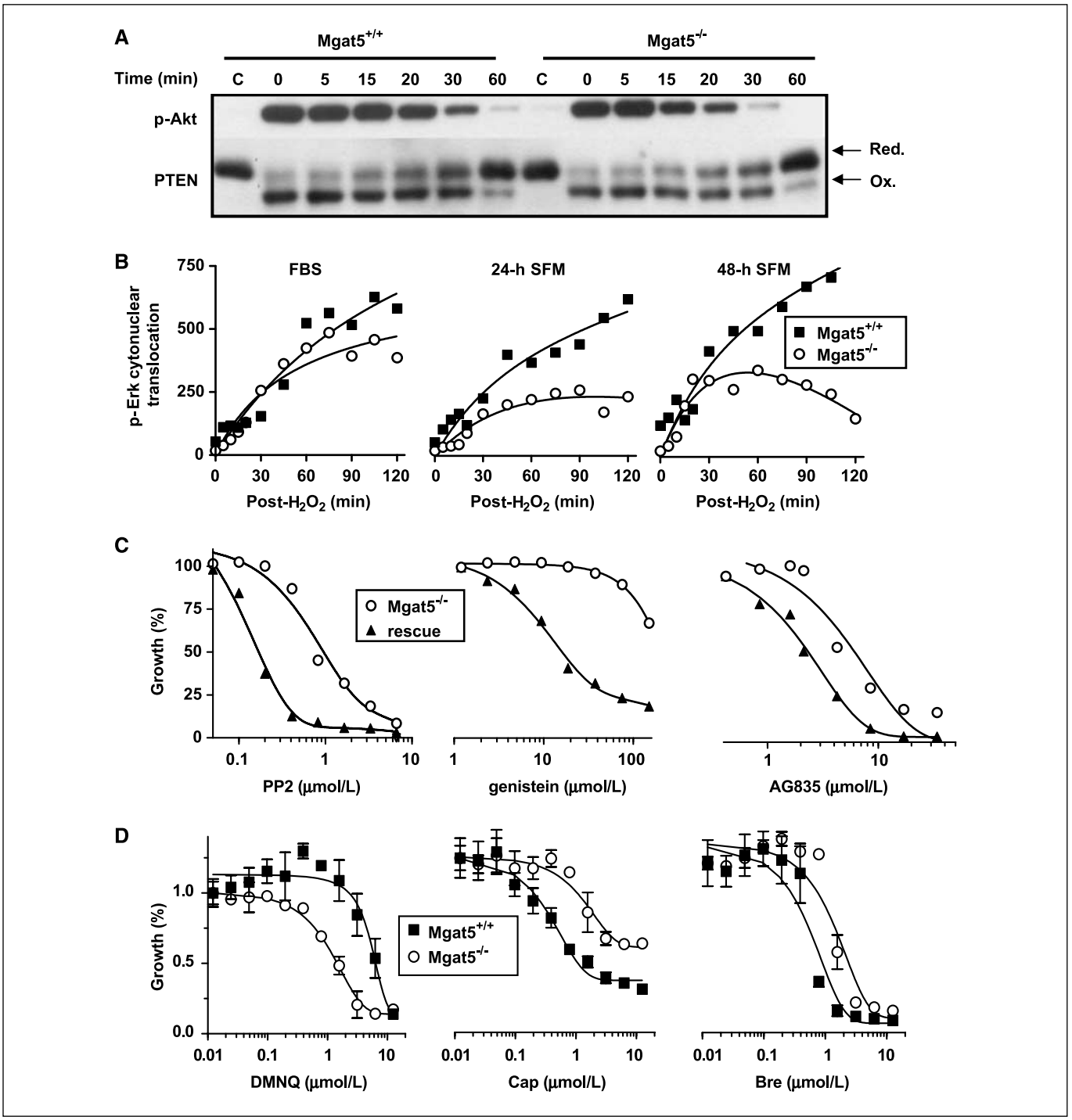

Figure 5. Redox turnover of PTEN and Erk/Akt signaling in tumor cells. *A,* cells were serum starved for 24 h and then exposed to H_2O_2 for 20 min, and lysates were prepared for Western blotting with antibodies to p-Akt and PTEN. *Red.,* reduced; *Ox.,* oxidized. *B,* time course of p-Erk nuclear-cytoplasmic difference in Mgat5$^{+/+}$ and Mgat5$^{-/-}$ tumor cells following a 30-min pulse of 1 mmol/L H_2O_2. *C,* sensitivity of Mgat5$^{-/-}$ and Mgat5-rescued Mgat5$^{-/-}$ cells to PP2, genistein, and AG835. Cells were cultured in the presence of the drug for 4 d in DMEM plus 1% FBS. *D,* differential sensitivity of Mgat5$^{+/+}$ and Mgat5$^{-/-}$ cells to three compounds identified in a screen of the Sigma LOPAC(1280) chemical library conducted in DMEM plus 1% FBS. *Points,* mean of three experiments; *bars,* SD. *Cap,* camptothecin; *Bre,* brefeldin A.

pathways in transformed cells increases Mgat4, Mgat5, and β1,3N-acetylglucosaminyltransferase expression (35–37), which reduces the apparent D_{50} of the pathway for UDP-GlcNAc. This effectively decreases the sensitivity of pathway end products to UDP-GlcNAc below estimated physiologic concentration of ~1.5 mmol/L (8).

Surface levels of TβR in Mgat5$^{-/-}$ were lower than Mgat5$^{+/+}$ cells, and GlcNAc supplementation increased TβR to comparable levels for both cell lines (Supplementary Fig. S3*B*). Surface levels of EGFR were partially rescued in Mgat5$^{-/-}$ cells by GlcNAc supplementation (8), and acute responsiveness to both EGF and TGF-β was largely restored (Supplementary Fig. S3*C* and *D*). Thus, an increase in the less branched tri-antennary *N*-glycans is sufficient to restore the surface residency of receptors in Mgat5$^{-/-}$ cells. Importantly, GlcNAc supplementation normalized glucose and ROS transport in Mgat5$^{-/-}$ cells under low serum conditions (Fig. 6*A*).

GlcNAc suppressed the growth of Mgat5$^{-/-}$ tumor cells to a greater degree than Mgat5$^{+/+}$ tumor cells (Fig. 6*B*; Supplementary Fig. S4*A–C*). Mgat5$^{-/-}$ tumor cells displayed a higher proportion of S-phase cells, and GlcNAc supplementation at 20 to 30 mmol/L rescued the cell cycle profile. However, higher concentrations of GlcNAc selectively suppressed proliferation of Mgat5$^{-/-}$ cells compared with Mgat5$^{+/+}$ cells (Fig. 6*B*; Supplementary Fig. S4*A–C*). The cell cycle profile in Mgat5$^{+/+}$ cells was less severely affected by GlcNAc, with only a small increase in the S-phase population. GlcNAc supplementation restored basal nuclear phospho-Smad2/3 (p-Smad2/3) in Mgat5$^{-/-}$ cells to levels comparable with that of Mgat5$^{+/+}$ cells, presumably reflecting enhanced sensitivity to autocrine/paracrine TGF-β. Similarly,

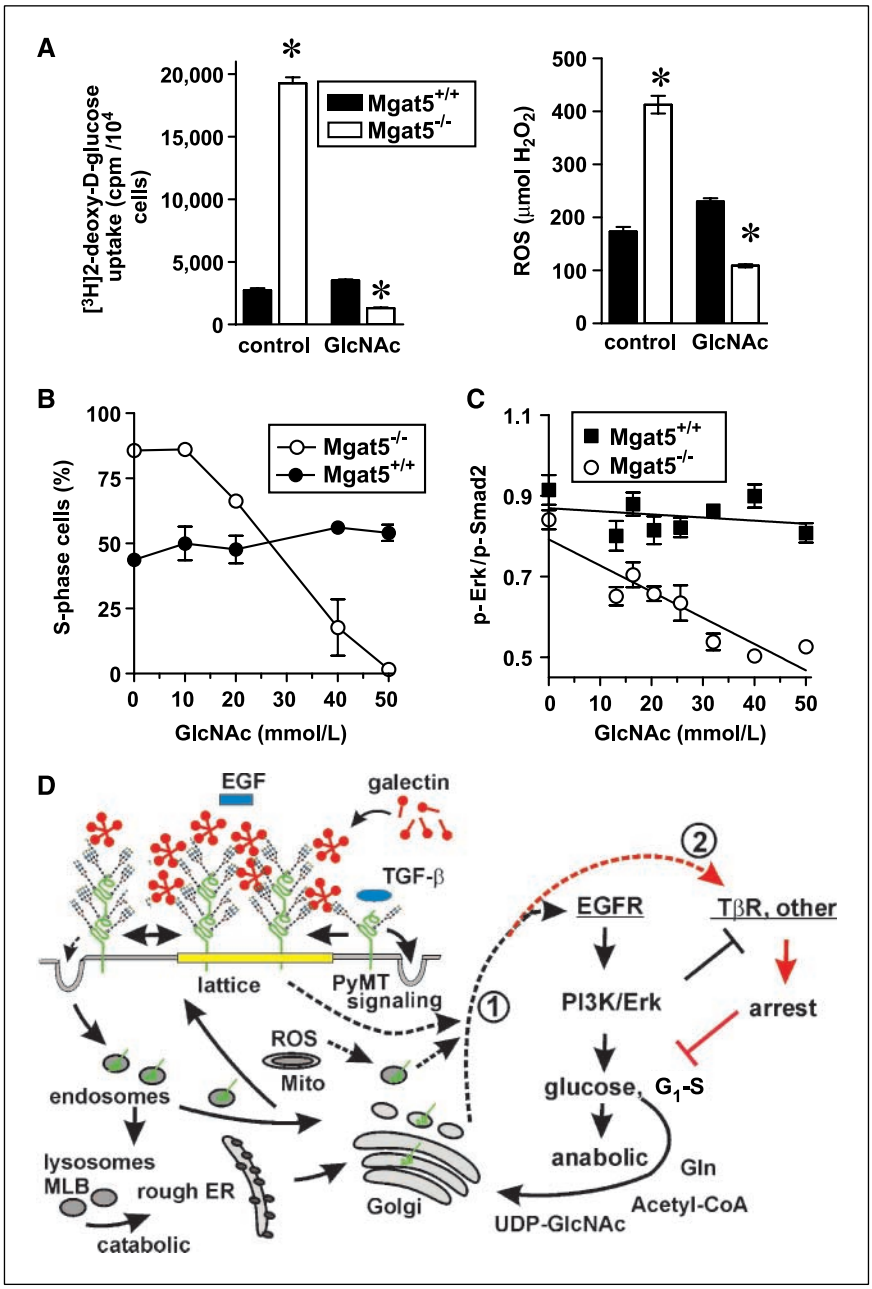

Figure 6. Mgat5 balances hexosamine-dependent regulation of metabolism and tumor cell proliferation. *A,* [^{3}H]2-deoxy-D-glucose uptake and ROS levels for Mgat5$^{+/+}$ and Mgat5$^{-/-}$ tumor cells cultured in DMEM plus 10% FBS for 48 h either with or without 40 mmol/L GlcNAc, followed by 24 h in SFM. *B,* S-phase fraction by FACS analysis for Mgat5$^{+/+}$ and Mgat5$^{-/-}$ cells cultured in DMEM plus 10% FBS supplemented with GlcNAc for 48 h (cell cycle distribution is in Supplementary Fig. S4). *C,* tonic levels of nuclear p-Erk and p-Smad2 expressed as a ratio in Mgat5$^{+/+}$ and Mgat5$^{-/-}$ cells following 48 h of GlcNAc supplementation in normal growth conditions. *D,* a model of *N*-glycan–dependent regulation of cytokine receptors and metabolism. The PyMT oncoprotein directly activates PI3K/Akt, promoting positive feedback to glucose uptake. Glucose metabolism increases ROS, thus oxidation of signaling intermediates that stimulate growth. Metabolic flux to the hexosamine and *N*-glycan branching pathway and/or Mgat5 expression increases affinities for galectin and surface residency of cytokine receptors in a lattice microdomain (see ref. 8). RTKs that promote growth have relatively high numbers of *N*-glycans with 11.4 ± 5.1 N-X-S/T consensus sequences (n = 30 receptor) and estimated to be ~70% occupancy. Receptor kinases with low multiplicity function in organogenesis and differentiation/arrest include Tie1, Musk, Ltk, ROR1/2, DDR1, the Eph receptors, and TGF-β/BMP receptors (27 receptors 2.48 ± 1.28 N-X-S/T sites/receptor). In Mgat5$^{-/-}$ cells, insufficient positive feedback from the cell surface (*1*) is partially alleviated by ROS-dependent activation of growth signaling intermediates (*green*) in the endosomes. However, positive feedback via the hexosamine/*N*-glycan processing is also insufficient to maintain (*2*) TβR and other low receptors with few *N*-glycans at levels sufficient to retrain the cell cycle. In PyMT Mgat5$^{+/+}$ cells, RTKs attain higher affinities for galectins and are retained at the cell surface in greater numbers and dominate over TβR and other low receptors.

GlcNAc partially restored basal nuclear p-Erk in serum-depleted conditions (Supplementary Fig. S3*C* and *D*). In culture conditions with serum, the ratio of p-Erk to p-Smad2/3 in Mgat5$^{-/-}$ cells decreased with GlcNAc supplementation but much less in Mgat5$^{+/+}$ cells (Fig. 6*C*). TGF-β/Smad and PI3K/Erk pathways are antagonistic at multiple levels (5, 38) and therefore likely to play a role in growth control as has been observed in *Caenorhabditis elegans* (39). Our results show that Mgat5 products, the β1,6GlcNAc-branched *N*-glycans, are required to balance growth and arrest signaling in PyMT tumor cells (Fig. 6*D*).

Discussion

Tumor progression in PyMT transgenic mice is slower in Mgat5$^{-/-}$ mice than in WT mice, and Mgat5$^{-/-}$ mammary tumor cells established in tissue culture are deficient in responsiveness to multiple ligands (7, 12). Tonic levels of activated p-Erk, p-Akt, ATP, and protein synthesis under normal culture conditions were comparable in Mgat5$^{-/-}$ and Mgat5$^{+/+}$ tumor cells, but surprisingly, removal of serum failed to suppress glucose metabolism, protein synthesis, and ROS production in Mgat5$^{-/-}$ tumor cells. Elevated ROS and Akt activation in Mgat5$^{-/-}$ tumor cells is dependent on glucose metabolism because chemical uncoupling of oxidative respiration normalized both. Mutant cells displayed an accelerated turnover of p-Erk and p-Akt, possibly due to parallel increases in ROS production and anti-oxidant activities. Rapamycin reduced ROS and glucose uptake in Mgat5$^{-/-}$ tumor cells, indicating a requirement for positive feedback through mTOR. Thus, sustained glucose uptake and mitochondrial ROS production in PyMT Mgat5$^{-/-}$ tumor cells promotes Akt and Erk signaling. The elevated energy charge in Mgat5$^{-/-}$ tumor is expected to suppress negative regulation of mTOR/S6K by AMPK (40). Indeed, depletion of S6K1 or mutation of the S6K phosphorylation sites in S6 decreases cell size and increases protein synthesis rates, similar in this regard to the phenotype of the PyMT Mgat5$^{-/-}$ tumor cells (41). Interestingly, nutrient restriction in *Drosophila* AMPKα-deficient epithelial cells results in loss of polarity and overproliferation, suggesting that changes in basic metabolism are an important aspect of the cancerous phenotype (42). ROS has been shown to activate mTOR in cultured human cells, whereas S6K1 phosphorylation becomes insensitive to nutrient deprivation (43). We suggest that ROS-dependent growth signaling and changes in metabolite flux to *N*-glycan biosynthesis may be critical determinants of cell size and growth autonomy.

Activation of EGFR at the plasma membrane by EGF stimulates PI3K/Akt signaling and H_2O_2 production via Rac1/NOX in a transient and localized manner that promotes polarization of microfilaments and cell motility (13). In contrast, ROS generated by the electron transport chain is likely to be persistent, and nonpolarized, as mitochondria are generally distributed in the cell. Moreover, activation of EGFR by H_2O_2 or EGF induces different patterns of receptor phosphorylation, which can affect signaling dynamics. The c-Cbl binding site at Tyr^{1045} is under phosphorylation by H_2O_2 stimulation, whereas four other sites common to EGFR stimulation are phosphorylated. As such, H_2O_2 prolongs EGFR activation by slowing ubiquitination and transit to the endosomes where inactivation occurs by PTPs (44). Near saturating levels of phosphatase activities are required to maintain the sensitivity of cytokine receptors to ligands. For example, EGFR is under tonic phosphatase suppression in endomembrane compartments, but redox-dependent suppression of PTPs in the endosomes promotes ligand-independent activation (13, 14). Elevated ROS in Mgat5$^{-/-}$ tumor cells may favor tonic activation of RTKs present at higher levels in endosomes (7). Mgat5$^{-/-}$ tumor cells are more resistant to Src and EGFR kinase inhibitors and to brefeldin A, an inhibitor of guanine nucleotide-exchange proteins (BIG) for ADP-ribosylation factors, which are required in Golgi vesicular transport (45). The relative resistance of Mgat5$^{-/-}$ tumor cells to these drugs is consistent with a reduced requirement for surface expression of growth factor receptors.

PyMT Mgat5$^{-/-}$ cells are checkpoint deficient and display an abnormal cell cycle distribution. PI3K/Akt activity normally increases at G_1-S, then declines with the G_2 pause, and increases again at G_2-M (26). Apparently, high levels of metabolic ROS in PyMT Mgat5$^{-/-}$ cells blocks the down-regulation of Akt in G_2 and hastens M phase. Consistent with loss of checkpoints and high ROS, PyMT Mgat5$^{-/-}$ tumor cells are relatively resistant to genotoxic agents and sensitive to DMNQ, a ROS inducer. However, oxidative stress also stimulates acetylation and activation of FOXO and p53 (46, 47), which drives expression of checkpoint, DNA repair, and anti-oxidant proteins, including GADD45, cyclin B, plk1, mSOD, and p27^{Kip1} (48). Of these competing effects, glucose metabolism and checkpoint dysfunction prevail in PyMT Mgat5$^{-/-}$ tumor cells, suggesting that Mgat5-modifed *N*-glycans are required for growth arrest. On serum withdrawal, PyMT Mgat5$^{-/-}$ tumor cells fail to down-regulate glucose metabolism and ROS, but both are down-regulated in primary MEFs, and to a greater extent in the Mgat5$^{-/-}$ MEFs. This argues that growth stimulation by PyMT oncoprotein promotes glucose transport, metabolic ROS, and positive feedback to growth signaling, compensating in part for loss of growth factor sensitivity in Mgat5$^{-/-}$ cells.

Both GlcNAc supplementation and Mgat5 expression promote receptor binding to galectins and shift receptor residency from the endosomes (ROS-dependent RTKs) to the cell surface (ligand dependent), but with qualitative differences. GlcNAc supplementation fully rescued surface TβRII receptor, which has only two *N*-glycans, whereas EGFR with eight *N*-glycans remains partially dependent on Mgat5 for optimal hexosamine-dependent surface expression (8).

In keeping with this relationship, increasing GlcNAc supplementation reduced the nuclear p-Erk/p-Smad2/3 ratio in Mgat5$^{-/-}$ tumor cells, as well as glucose uptake and proliferation, whereas GlcNAc had a more modest effect on Mgat5$^{+/+}$ cells (Fig. 6*D*). Mgat5 expression commonly increases in oncogene-transformed cells, and predictions based on computational modeling indicate that Mgat5 products preferentially increase the surface levels of growth receptors (high number of *N*-glycans), relative to TβRII and other glycoproteins with few *N*-glycans (8). Our results suggest that nutrient flux to complex *N*-glycan biosynthesis coordinates the cellular response to multiple extracellular cues in tumor cells that determine growth, invasion, and sensitivity to drugs.

Acknowledgments

Received 12/12/2006; revised 5/25/2007; accepted 7/6/2007.

Grant support: Canadian Institutes of Health Research (CIHR) and Genome Canada through the Ontario Genomics Institute (J.W. Dennis) and a CIHR studentship (E. Partridge).

The costs of publication of this article were defrayed in part by the payment of page charges. This article must therefore be hereby marked *advertisement* in accordance with 18 U.S.C. Section 1734 solely to indicate this fact.

We thank Dr. Jeff L. Wrana for helpful discussion.

References

1. Thiery JP. Epithelial-mesenchymal transitions in development and pathologies. Curr Opin Cell Biol 2003;15:740–6.
2. Di Paolo G, De Camilli P. Phosphoinositides in cell regulation and membrane dynamics. Nature 2006;443:651–7.
3. Ozdamar B, Bose R, Barrios-Rodiles M, et al. Regulation of the polarity protein Par6 by TGFβ receptors controls epithelial cell plasticity. Science 2005;307:1603–9.
4. Seoane J, Le HV, Shen L, Anderson SA, Massague J. Integration of Smad and forkhead pathways in the control of neuroepithelial and glioblastoma cell proliferation. Cell 2004;117:211–23.
5. Matsuura I, Denissova NG, Wang G, et al. Cyclin-dependent kinases regulate the antiproliferative function of Smads. Nature 2004;430:226–31.
6. Oft M, Akhurst RJ, Balmain A. Metastasis is driven by sequential elevation of H-ras and Smad2 levels. Nat Cell Biol 2002;4:487–94.
7. Partridge EA, Le Roy C, Di Guglielmo GM, et al. Regulation of cytokine receptors by Golgi *N*-glycan processing and endocytosis. Science 2004;306:120–4.
8. Lau K, Partridge EA, Silvescu CI, et al. Complex *N*-glycan number and degree of branching cooperate to regulate cell proliferation and differentiation. Cell 2007;129:123–4.
9. Grigorian A, Lee S-U, Tian W, et al. Control of T cell mediated autoimmunity by metabolite flux to *N*-glycan biosynthesis. J Biol Chem 2007;282:20027–35.
10. Sasai K, Ikeda Y, Fujii T, Tsuda T, Taniguchi N. UDP-GlcNAc concentration is an important factor in the biosynthesis of β1,6-branched oligosaccharides: regulation based on the kinetic properties of *N*-acetylglucosaminyltransferase V. Glycobiology 2002;12:119–27.
11. Webster MA, Hutchinson JN, Rauh MJ, et al. Requirement for both Shc and phosphatidylinositol 3′ kinase signaling pathways in polyomavirus middle T-mediated mammary tumorigenesis. Mol Cell Biol 1998;18:2344–59.
12. Granovsky M, Fata J, Pawling J, et al. Suppression of tumor growth and metastasis in Mgat5-deficient mice. Nat Med 2000;6:306–12.
13. Reynolds AR, Tischer C, Verveer PJ, Rocks O, Bastiaens PI. EGFR activation coupled to inhibition of tyrosine phosphatases causes lateral signal propagation. Nat Cell Biol 2003;5:447–53.
14. Offterdinger M, Georget V, Girod A, Bastiaens PI. Imaging phosphorylation dynamics of the epidermal growth factor receptor. J Biol Chem 2004;279:36972–81.
15. den Hertog J, Groen A, van der Wijk T. Redox regulation of protein-tyrosine phosphatases. Arch Biochem Biophys 2005;434:11–5.
16. Salmeen A, Andersen JN, Myers MP, et al. Redox regulation of protein tyrosine phosphatase 1B involves a sulphenyl-amide intermediate. Nature 2003;423:769–73.
17. Lee SR, Yang KS, Kwon J, et al. Reversible inactivation of the tumor suppressor PTEN by H_2O_2. J Biol Chem 2002;277:20336–42.
18. Nimnual AS, Taylor LJ, Bar-Sagi D. Redox-dependent downregulation of Rho by Rac. Nat Cell Biol 2003;5:236–41.
19. Sundaresan M, Yu ZX, Ferrans VJ, Irani K, Finkel T. Requirement for generation of H_2O_2 for platelet-derived growth factor signal transduction. Science 1995;270:296–9.
20. Park HS, Lee SH, Park D, et al. Sequential activation of phosphatidylinositol 3-kinase, β Pix, Rac1, and Nox1 in growth factor-induced production of H_2O_2. Mol Cell Biol 2004;24:4384–94.
21. Radisky DC, Levy DD, Littlepage LE, et al. Rac1b and reactive oxygen species mediate MMP-3-induced EMT and genomic instability. Nature 2005;436:123–7.
22. Echtay KS, Roussel D, St-Pierre J, et al. Superoxide activates mitochondrial uncoupling proteins. Nature 2002;415:96–9.
23. Kim JH, Chu SC, Gramlich JL, et al. Activation of the PI3K/mTOR pathway by BCR-ABL contributes to increased production of reactive oxygen species. Blood 2005;105:1717–23.
24. Suh YA, Arnold RS, Lassegue B, et al. Cell transformation by the superoxide-generating oxidase Mox1. Nature 1999;401:79–82.
25. Weinstein J, Sundaram S, Wang X, et al. A point mutation causes mistargeting of Golgi GlcNAc-TV in the Lec4A Chinese hamster ovary glycosylation mutant. J Biol Chem 1996;271:27462–9.
26. Roberts EC, Shapiro PS, Nahreini TS, et al. Distinct cell cycle timing requirements for extracellular signal-regulated kinase and phosphoinositide 3-kinase signaling pathways in somatic cell mitosis. Mol Cell Biol 2002;22:7226–41.
27. Vander Heiden MG, Plas DR, Rathmell JC, et al. Growth factors can influence cell growth and survival through effects on glucose metabolism. Mol Cell Biol 2001;21:5899–912.
28. Macheda ML, Rogers S, Best JD. Molecular and cellular regulation of glucose transporter (GLUT) proteins in cancer. J Cell Physiol 2005;202:654–62.
29. Cheung P, Pawling J, Partridge EA, et al. Metabolic homeostasis and tissue renewal are dependent on β1,6GlcNAc-branched *N*-glycans. Glycobiology 2007;17:828–37.
30. Hahn-Windgassen A, Nogueira V, Chen CC, et al. Akt activates the mammalian target of rapamycin by regulating cellular ATP level and AMPK activity. J Biol Chem 2005;280:32081–9.
31. Ohanna M, Sobering AK, Lapointe T, et al. Atrophy of S6K1(−/−) skeletal muscle cells reveals distinct mTOR effectors for cell cycle and size control. Nat Cell Biol 2005;7:286–94.
32. Wang X, Li W, Williams M, et al. Regulation of elongation factor 2 kinase by p90(RSK1) and p70 S6 kinase. EMBO J 2001;20:4370–9.
33. McLeod LE, Proud CG. ATP depletion increases phosphorylation of elongation factor eEF2 in adult cardiomyocytes independently of inhibition of mTOR signalling. FEBS Lett 2002;531:448–52.
34. Kops GJ, Dansen TB, Polderman PE, et al. Forkhead transcription factor FOXO3a protects quiescent cells from oxidative stress. Nature 2002;419:316–21.
35. Buckhaults P, Chen L, Fregien N, Pierce M. Transcriptional regulation of *N*-acetylglucosaminyltransferase V by the src Oncogene. J Biol Chem 1997;272:19575–81.
36. Takamatsu S, Oguri S, Minowa MT, et al. Unusually high expression of *N*-acetylglucosaminyltransferase-IV a in human choriocarcinoma cell lines: a possible enzymatic basis of the formation of abnormal biantennary sugar chain. Cancer Res 1999;59:3949–53.
37. Ishida H, Togayachi A, Sakai T, et al. A novel β1,3-*N*-acetylglucosaminyltransferase (β3Gn-T8), which synthesizes poly-*N*-acetyllactosamine, is dramatically upregulated in colon cancer. FEBS Lett 2005;579:71–8.
38. Siegel PM, Massague J. Cytostatic and apoptotic actions of TGF-β in homeostasis and cancer. Nat Rev Cancer 2003;3:807–21.
39. Morita K, Flemming AJ, Sugihara Y, et al. A *Caenorhabditis elegans* TGF-β, DBL-1, controls the expression of LON-1, a PR-related protein, that regulates polyploidization and body length. EMBO J 2002;21:1063–73.
40. Reiling JH, Sabatini DM. Stress and mTORture signaling. Oncogene 2006;25:6373–83.
41. Ruvinsky I, Sharon N, Lerer T, et al. Ribosomal protein S6 phosphorylation is a determinant of cell size and glucose homeostasis. Genes Dev 2005;19:2199–211.
42. Mirouse V, Swick LL, Kazgan N, St Johnston D, Brenman JE. LKB1 and AMPK maintain epithelial cell polarity under energetic stress. J Cell Biol 2007;177:387–92.
43. Sarbassov DD, Sabatini DM. Redox regulation of the nutrient-sensitive raptor-mTOR pathway and complex. J Biol Chem 2005;280:39505–9.
44. Ravid T, Sweeney C, Gee P, Carraway KL III, Goldkorn T. Epidermal growth factor receptor activation under oxidative stress fails to promote c-Cbl mediated down-regulation. J Biol Chem 2002;277:31214–9.
45. Shen X, Hong MS, Moss J, Vaughan M. BIG1, a brefeldin A-inhibited guanine nucleotide-exchange protein, is required for correct glycosylation and function of integrin β_1. Proc Natl Acad Sci U S A 2007;104:1230–5.
46. Brunet A, Sweeney LB, Sturgill JF, et al. Stress-dependent regulation of FOXO transcription factors by the SIRT1 deacetylase. Science 2004;303:2011–5.
47. Essers MA, de Vries-Smits LM, Barker N, et al. Functional interaction between β-catenin and FOXO in oxidative stress signaling. Science 2005;308:1181–4.
48. Tran H, Brunet A, Grenier JM, et al. DNA repair pathway stimulated by the forkhead transcription factor FOXO3a through the Gadd45 protein. Science 2002;296:530–4.

Complex *N*-Glycan and Metabolic Control in Tumor Cells

Richard Mendelsohn, Pam Cheung, Lloyd Berger, et al.

Cancer Res 2007;67:9771-9780.